APPLICATION OF DEM-BASED ANALYSIS IN THE OPTIMIZATION OF SHOVEL DESIGN FOR THE 1JS-200 ROCK PICKER

/

基于离散元法的 1JS-200 型捡石机起石铲的优化设计应用

Yasenjiang BAIKELI *[1,2], Jiaxi ZHANG [1,2], Jihuai GAO [3]; Haodong XU [1,2]

[1] College of Mechanical and Electrical Engineering, Xinjiang Agricultural University, Urumqi/ China;

[2] Key Laboratory of Xinjiang Intelligent Agricultural Equipment, Urumqi / China;

[3] Xinjiang Dafengge Agricultural Machinery Co., LTD, Bole / China;

Tel: 8613899827528; E-mail: yasin@zju.edu.cn

Corresponding author: Yasenjiang Baikeli

DOI: https://doi.org/10.35633/inmateh-76-56

Keywords: *Discrete element Method, Rock Picker, Shovel, Interaction, Optimization*

ABSTRACT

To enhance the operational efficiency and structural design accuracy of rock-picking machinery, this study proposes a Discrete Element Method (DEM)-based approach for the optimization of the lifting shovel in the 1JS-200 rock picker. A coupling simulation model of the shovel-soil-rock system was established to analyze the dynamic interaction mechanisms between the shovel and mixed granular media. Key parameters influencing excavation performance-including forward speed, digging depth, and shovel angle-were optimized using a Box-Behnken Design (BBD) response surface methodology. Regression models were constructed for torque and rock excavation efficiency (REE), and the optimal combination was determined to be a forward speed of 0.5 m/s, a digging depth of 170 mm, and a shovel angle of 40°, under which the predicted REE reached 88.1% with a torque of approximately 386 N·m. To validate the simulation results, field tests were conducted under optimal parameter conditions. The experimental results showed that REE values fluctuated within 2%, and torque errors remained within 4% of the predicted values, confirming the accuracy and applicability of the model. This research provides a practical, data-driven design method for rock-picking implements and offers theoretical and technical support for improving rock separation efficiency, reducing structural wear, and advancing the intelligent development of agricultural machinery.

摘要

为提升农田捡石机作业效率与结构设计的科学性，本文以 1JS-200 型捡石机的起石铲为对象，提出了一种基于离散元法（DEM）的结构优化方法。构建了起石铲–土壤–砾石系统的动力学模型，模拟分析了提升铲与混合颗粒介质之间的动态相互作用机制。在此基础上，采用 Box–Behnken 响应面设计方法，对作业速度、挖掘深度及铲角等关键参数进行优化，构建了扭矩与岩石清理效率（REE）的二次回归模型。结果表明，最优参数组合为作业速度 0.5 m/s、挖掘深度 170 mm、铲角 40°，在此条件下 REE 为 88.1%，扭矩约为 386 N·m。为验证模拟结果的可靠性，开展了田间验证试验。试验结果显示，实测 REE 波动范围控制在 2%，扭矩误差控制在 4%以内，验证了模型的准确性与适用性。研究成果为捡石作业设备的数据驱动式结构优化提供了实用路径，同时为提升捡石效率、降低设备磨损、推动农机装备智能化发展提供了理论依据与技术支撑。

INTRODUCTION

In modern agricultural mechanization, the widespread presence of rocks in farmland hinders operations like deep plowing, sowing, and harvesting, while accelerating wear and damage to machinery—ultimately limiting productivity and soil quality (*Mak & Chen, 2014*). Rock pickers are increasingly used in high-standard farmland construction, with the lifting shovel being the core component that directly affects rock-picking efficiency and machine stability. However, the 1JS-200 rock picker still suffers from low efficiency, high carryover, and severe wear, mainly due to its empirically driven design and lack of systematic analysis of the shovel's dynamic interaction with the soil–rock mixture under varying field conditions (*Coetzee, 2009; Fielke & Ucgul, 2013; Servin et al., 2020*). To address this, the Discrete Element Method (DEM) offers a robust approach to simulate shovel–material interactions and guide structural optimization (*Mak & Chen, 2014*).

***[1,2]** *Yasenjiang Baikeli, Ph.D.Eng.;* [1,2] *Jiaxi Zhang, Prof.Ph.D.Eng.,*[3] *Jihuai Gao, Prof.Eng.;* [1,2] *Haodong Xu, M.S.Stud.Eng.*

Applying DEM to the 1JS-200 shovel structure is therefore essential for enhancing rock removal efficiency, improving machine intelligence, and advancing high-quality agricultural development.

In recent years, significant progress has been made in the simulation and design of soil-engaging tools through the application of the Discrete Element Method (DEM) and data-driven optimization techniques. For instance, *Franco et al. (2007*) and *Shmulevich et al. (2007)* made important contributions by using DEM to analyze the interaction between soil and bulldozer blades or wide cutting tools. Their work laid a theoretical foundation for modeling soil-tool contact mechanics and demonstrated the applicability of DEM in agricultural engineering. However, these studies primarily considered homogeneous soil conditions and simplified tool geometries, and they did not account for the coupled interactions between soil, rocks, and shovel surfaces. As a result, they fell short in capturing the complex dynamic behavior that occurs during rock-picking operations.

In terms of structural optimization, researchers such as *Zhang & Li*, *(2024)* successfully applied response surface methodologies to optimize tillage tool parameters, providing a more quantitative alternative to traditional trial-and-error approaches. Their studies demonstrated the effectiveness of Box–Behnken Design (BBD) and multi-factor analysis in improving tool performance. Nevertheless, most of these applications focused on relatively simple soil conditions and low-load scenarios. For high-resistance components such as lifting shovels in rock-picking equipment, the optimization process remains largely experience-based, lacking systematic multi-parameter analysis tailored to the mechanical demands of mixed soil–rock environments. Furthermore, there has been increasing interest in bridging the gap between virtual simulation and real-world testing. *Shmulevich et al. (2007)* and *Rizzardo et al. (2020)* explored virtual testing frameworks and discussed the limitations of simulation-to-reality (Sim2Real) transfer in agricultural machinery and robotics. These studies emphasized the importance of validation, but many existing works still treat simulation and field testing as separate processes. This often leads to discrepancies between predicted and actual performance, limiting the reliability and practical value of the models in field-scale applications such as rock separation under variable terrain and load conditions.

To overcome these limitations, this study proposes an integrated simulation and optimization framework for analyzing shovel-soil-rock interactions in rock-picking operations. A coupled modeling approach based on the Discrete Element Method (DEM) is developed to dynamically simulate the interaction between the lifting shovel and complex granular media, offering theoretical insight into the underlying mechanical processes. A structural optimization strategy using the Box–Behnken Design (BBD) is employed to systematically evaluate the influence of key parameters-such as operating speed, digging depth, and shovel angle-on performance. In addition, a performance verification method is established to validate the simulation results. This research not only enhances the theoretical methodology for agricultural equipment design optimization but also provides technical support for improving rock-picking efficiency, minimizing equipment wear, and advancing the intelligent development of rock-clearing machinery.

MATERIALS AND METHODS

Description of the 1JS-200 Rock Picker

The 1JS-200 is a chain-type rock picker designed for excavating, conveying, and collecting stones in agricultural fields. Its main structural parameters are listed in Table 1. As shown in Figure 1, the machine is composed of a towing frame *1*, rock-lifting shovel *2*, ground wheels *3*, stone collection box *4*, stone conveying mechanism *5* and chain drive system *6*.

During operation, the rock picker is towed forward by a tractor. The shovel cuts into the soil to dislodge stones, which are then lifted and conveyed via a chain-driven belt to the rear collection unit. The system is designed to separate larger stones from the soil while allowing finer particles to fall through during transport. The ground wheels provide mobility across varying field conditions.

The shovel is the key component responsible for stone excavation and directly affects the machine's overall efficiency. However, its current design faces challenges such as shallow digging capacity, instability on uneven terrain, and inefficient separation of stones from soil. These issues motivate the need for design optimization, where DEM-based analysis can be applied to simulate material interaction and improve performance.

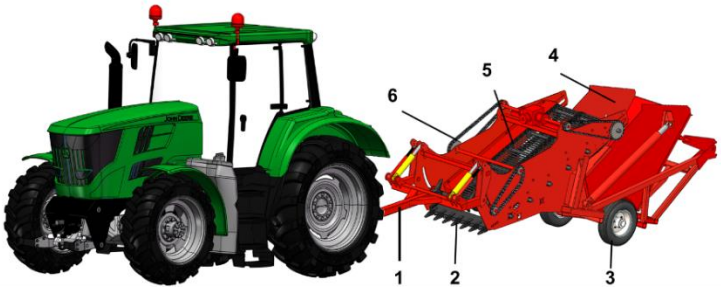

Fig. 1 - 1JS-200 Rock Picker Machine

Table 1

Discrete element model parameters of

Serial	Parameter	Value
1	Overall dimensions (L × W × H)	6250×1750×2150 mm
2	Structural weight	3500 kg
3	Required power	>40.5 KW (≥ 55 hp)
4	Working width	1300 mm
5	Suitable stone size range	600~700 mm
6	Operating speed	<5 km/h
7	Stone removal efficiency	>80 %

Shovel-Soil-Rock Interaction Modeling

Simulating shovel interactions with complex terrains composed of soil and embedded rocks presents challenges for conventional modeling methods, which often fail to capture the discrete, nonlinear behavior of granular media (*Servin, Berglund, & Nystedt, 2020*). The Discrete Element Method (DEM) offers a more suitable approach by modeling particle-scale interactions and contact dynamics, making it ideal for analyzing excavation processes in heterogeneous field conditions (*Coetzee, 2017*).

To simulate the mechanical behavior of multi-phase terrain during excavation, a discrete element modeling (DEM) framework was developed to represent the interaction between shovel tools, soil particles, and embedded rocks. As illustrated in Fig. 2, the modeling workflow begins with the physical characterization of soil and scattered surface rocks (Fig. 2a). These physical rock entities are digitally reconstructed, yielding a range of geometric types-spherical, irregular, and ellipsoidal shapes-to reflect natural variability (Fig. 2b). To balance geometric realism with computational efficiency, these three representative rock shapes were selected. This combination captures the essential morphological diversity observed in field conditions while ensuring manageable simulation complexity within the DEM framework. The final DEM framework integrates the reconstructed rock particles into a densely packed soil matrix and simulates the dynamic interaction as the shovel penetrates the terrain (Fig.2c). The model captures key behaviors such as contact force propagation, material displacement, and rock–soil separation. This enables quantitative evaluation of shovel performance under unstructured, heterogeneous field conditions and supports informed design optimization.

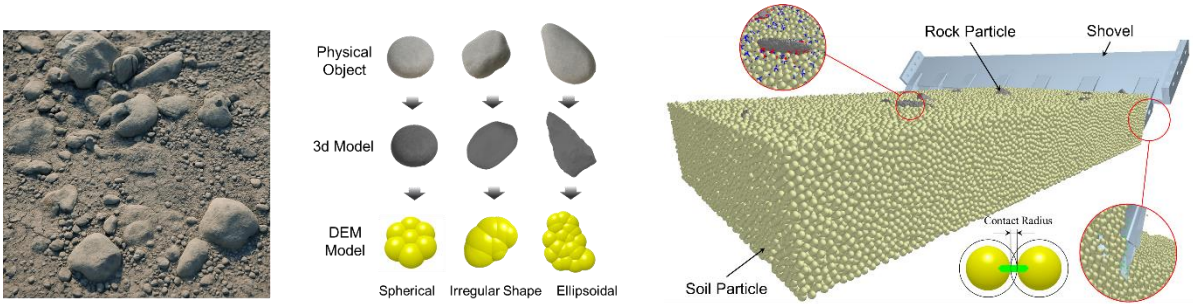

(a) Land of Soil - Rocks *(b) Modeling Process of Rocks* *(c) DEM Model of Shovel-Soil-Rock*

Fig. 2 - Discrete Element Model of Shovel-Soil-Rock Interaction

All parameters required for establishing the discrete element model in this section are set according to Table 2, where the contact parameters of the lifting shovel - soil - rocks (collision recovery coefficient, static friction coefficient, rolling friction coefficient) are obtained from the calibration tests and existing research literature, and other parameters are set with reference to previous studies.

Table 2

Discrete element model parameters

Type	Parameter	Value	Unit	Ref.
Rock	Density	2,500	kg/m³	*Zou et al., (2020); Camborde et al., (2000)*
	Young's Modulus	5.0E+10	Pa	*Zou et al., (2020); Camborde et al., (2000)*
	Poisson's Ratio	0.3	-	*Zou et al., (2020); Camborde et al., (2000)*
	Normal Stiffness	1.0E+7	N/m	*Zou et al., (2020); Camborde et al., (2000)*
	Tangential Stiffness	1.0E+6	N/m	*Zou et al., (2020); Camborde et al., (2000)*
	Friction Coefficient	0.4	-	*Zou et al., (2020); Camborde et al., (2000)*
Soil	Density	1,600	kg/m³	*Horn, (2004); Mak & Chen, (2014)*
	Young's Modulus	2.0E+7	Pa	*Horn, (2004); Mak & Chen, (2014)*
	Poisson's Ratio	0.35	-	*Horn, (2004); Mak & Chen, (2014)*
	Normal Stiffness	5.0E+6	N/m	*Horn, (2004); Mak & Chen, (2014)*
	Tangential Stiffness	5.0E+5	N/m	*Horn, (2004); Mak & Chen, (2014)*
	Friction Coefficient	0.35	-	*Horn, (2004); Mak & Chen, (2014)*
Shovel (Q235 Steel)	Density	7,850	kg/m³	*Feng et al., (2022); Zhang et al., (2023)*
	Young's Modulus	2.1E+11	Pa	*Feng et al., (2022); Zhang et al., (2023)*
	Poisson's Ratio	0.3	-	*Feng et al., (2022; Zhang et al., (2023)*
	Normal Stiffness	2.1E+11	N/m	*Feng et al., (2022); Zhang et al., (2023)*
	Tangential Stiffness	2.1E+10	N/m	*Feng et al., (2022); Zhang et al., (2023)*
	Friction Coefficient	0.3	-	*Feng et al., (2022); Zhang et al., (2023)*
Soil–Rock	Normal Stiffness	5.0E+6	N/m	*Zou et al., (2020)*
	Tangential Stiffness	5.0E+5	N/m	*Zou et al., (2020)*
	Friction Coefficient	0.35	-	*Zou et al., (2020)*
Shovel–Rock	Normal Stiffness	1.0E+8	N/m	*Fielke et al., (2013); Feng et al., (2022)*
	Tangential Stiffness	1.0E+7	N/m	*Fielke et al., (2013); Feng et al., (2022)*
	Friction Coefficient	0.30	-	*Fielke et al., (2013); Feng et al., (2022)*
Shovel–Soil	Normal Stiffness	5.0E+7	N/m	*Mak & Chen, (2014); Zhang et al., (2023)*
	Tangential Stiffness	5.0E+6	N/m	*Mak & Chen, (2014); Zhang et al., (2023)*
	Friction Coefficient	0.28	-	*Mak & Chen, (2014); Zhang et al., (2023)*

Shovel-Soil-Rock models for Discrete Element Simulation Test

In order to accurately simulate the process of pulling rocks by the lifting shovel of the 1JS-200 rock picker and analyze the rock picking efficiency and torque, a simulation model of the lifting shovel-soil-rock interaction is constructed based on the discrete element method, as shown in Figure 3.

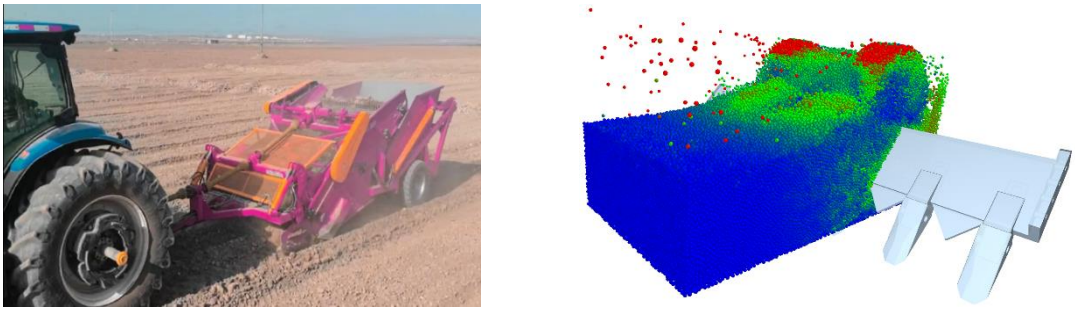

(a) Working View *(b) Shovel for DEM Simulation*

Fig. 3 - Discrete Element Simulation Model

Experimental Design and Performance Evaluation Methodology

Field experiments were conducted to test the operational effectiveness of the lifting shovel in the 1JS-200 rock picker under natural variability in the field. Fig 4(a) and Fig 4(b) show the structure and parameters of the Shovel, Fig 4(c) illustrates the interaction process between the lifting shovel**,** soil**,** and rock**.** As the lifting shovel moves forward, complex interactions occur between the shovel, soil particles, and rock particles.

The *V* in the figure represents the forward speed of the shovel, which directly impacts the disturbance caused to the soil and rock. *h* represents the digging depth, indicating the depth at which the shovel enters the soil, a critical factor affecting the soil-rock excavation efficiency. δ represents the angle between the shovel and the ground, which determines the direction of the forces acting on the soil and rock and the shovel's cutting behavior.

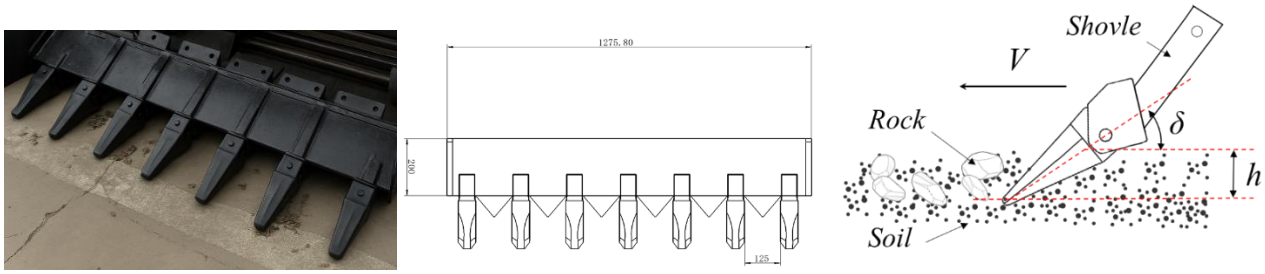

(a) Structure of Shovel *(b) Parameters of Shovel* *(c) Dynamic Parameters of Shovel*

Fig. 4 - Rock-Lifting Shovel

These conditions are of great significance to reduce experimental errors and ensure that the experimental results can be directly applied to improve the practical application performance of the rock picking device. In order to optimize the rock picking equipment, the effects of lifting shovel speed (X_1), digging depth (X_2), and angle (X_3) on the rock picking efficiency and operational torque were studied. Through Box-Behnken Design (BBD) experimental design, different speeds (X_1: 0.3 m/s to 0.7 m/s), digging depths (X_2: 160 mm to 200 mm), and angles (X_3: 30° to 50°) were set to simulate the interaction effects under different operating conditions. The experiment focused on recording the rock picking efficiency, operational torque, and evaluating the impact of X_1, X_2, and X_3 on performance. These results provide a reference basis for further optimizing the equipment. The selection of experimental factor levels is shown in Table 3.

Table 3

Experimental factor level design

Level	Factor		
	A (m/s)	B (mm)	C (°)
1	0.3	160	30
0	0.5	180	40
-1	0.7	200	50

Experimental Conditions and Performance Evaluation Metrics

To validate the effectiveness of the simulation-based optimization and evaluate the field performance of the 1JS-200 rock picker, a series of field experiments were conducted. The experimental site is located in Bole, Xinjiang, China (44.90° N, 81.69° E), within a typical farmland area commonly used for rock picking operations. The experimental equipment included the 1JS-200 rock picker, operated via a tractor, and the instrumentation focused on assessing rock excavation efficiency and operating torque under practical working conditions.

The field tests were designed in accordance with the Box-Behnken Design (BBD) optimization results. Key operating parameters-forward speed, digging depth, and shovel angle-were varied systematically within their respective ranges to evaluate their influence on performance metrics. Each test covered a fixed operation distance of 20 meters with a working width of 1.3 meters, as shown in Figure 5(a). These settings ensured comparable working volumes across trials, while still allowing the effects of the optimized parameters to be observed.

(a) Testing Field *(b) Torque Sensor*

Fig. 5 - Testing Field Method

After each trial, the total mass of collected rocks M_{rock} (*kg*) was measured using an electronic scale, and the operation time t (*s*) was recorded using a stopwatch. Operating torque and shaft speed were captured in real time using a Kistler Type 9051A rotary torque sensor installed on the machine's drive shaft, as shown in Figure 5(b). The average power *P* (*KW*) was calculated as:

$$P = \frac{T \cdot 2\pi \cdot RPM}{60 \times 1000} \quad (1)$$

Based on these measurements, the rock excavation efficiency (REE) was defined as the excavated rock mass per unit energy consumed:

$$REE = \frac{M_{rock}}{t \cdot P} \quad (2)$$

Each parameter combination was tested three times to ensure repeatability. The field conditions were consistent with typical rock picking scenarios in the region, and the empirical results provided robust validation for the DEM-based optimization strategy.

RESULTS AND ANALYSIS

Simulation process of Rock-Lifting

Figure 6 shows the cross-sectional DEM simulation of the shovel–soil–rock interaction at 1 s, 5 s, and 9 s. At 1 s (Fig. 6a), the shovel initiates penetration with minimal soil disturbance. By 5 s (Fig. 6b), particle displacement and velocity increase significantly near the shovel edge. At 9 s (Fig. 6c), high-velocity regions (>1.6 m/s) appear, indicating active excavation and effective rock-soil separation. The results highlight the dynamic interaction process and the shovel's influence on material flow.

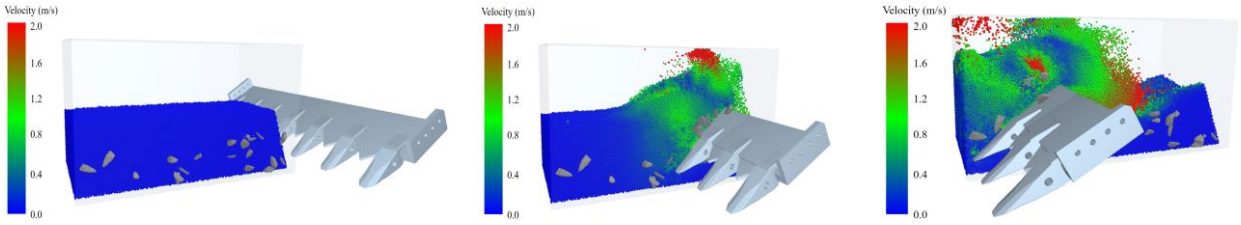

(a) 1 s *(b) 5 s* *(c) 9 s*

Fig. 6 - Cross-Sectional DEM Simulation of Shovel–Soil–Rock Interaction

Optimization Results Based on DEM and BBD Experiments

Discrete Element Method (DEM) simulations were conducted to analyze the influence of forward speed on the excavation performance of the 1JS-200 rock picker's shovel. Based on the Box-Behnken Design (BBD), three forward speeds were evaluated: 0.3 m/s, 0.5 m/s, and 0.7 m/s, while the other two parameters-digging depth and shovel angle-were held at their central values.

The simulation results, shown in Table 3, reveal a non-linear relationship between forward speed and rock excavation efficiency (REE). As the forward speed increases from 0.3 m/s to 0.5 m/s, the REE significantly improves, indicating enhanced soil-rock engagement and a more effective cutting-lifting interaction. At 0.5 m/s, the shovel achieves optimal contact with the soil-rock mixture, resulting in both high rock capture and relatively moderate energy consumption.

Table 4

Test factor level design

Serial Number	Forward speed (m/s)	REE (%)	Torque (N·m)
1	0.3	87.4	260.7
2	0.5	79.2	335.9
3	0.7	71.6	412.8

Three forward speeds were evaluated: 0.3 m/s, 0.5 m/s, and 0.7 m/s, as shown in Fig. 7. At 0.3 m/s (Fig. 7a), soil and rock movement is minimal, with most particles remaining in low-velocity zones (<0.4 m/s). At 0.5 m/s (Fig. 7b), material displacement increases, and a broader region of medium velocity (green) emerges. At the highest speed of 0.7 m/s (Fig. 7c), particle flow intensifies, with a clear expansion of high-velocity areas (>1.6 m/s) and increased rock-soil separation. These results suggest that higher operating speeds promote more efficient material disturbance, though potentially at the cost of increased energy input or wear.

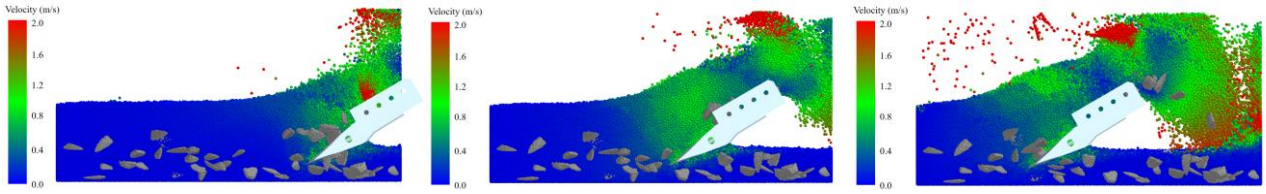

(a) v= 0.3 m/s *(b) v= 0.5 m/s* *(c) v= 0.7 m/s*

Fig. 7 – DEM Simulation of Soil and Rock Motion at Varying Shovel Speeds

Table 5

Test factor level design

Serial Number	Digging Depth (mm)	REE (%)	Torque (N·m)
1	160	82.6	310.3
2	180	79.2	335.9
3	200	75.4	362.1

As shown in Fig. 8, increasing the digging depth enhances shovel–rock contact, leading to greater rock displacement. At 160 mm, only shallow rocks are disturbed. At 180 mm, the shovel begins to lift embedded rocks, while at 200 mm, extensive rock separation occurs, indicating improved extraction. However, deeper excavation also increases soil disturbance and resistance. Thus, an optimal depth should balance rock-lifting efficiency and operational load, which can be determined through targeted DEM simulations.

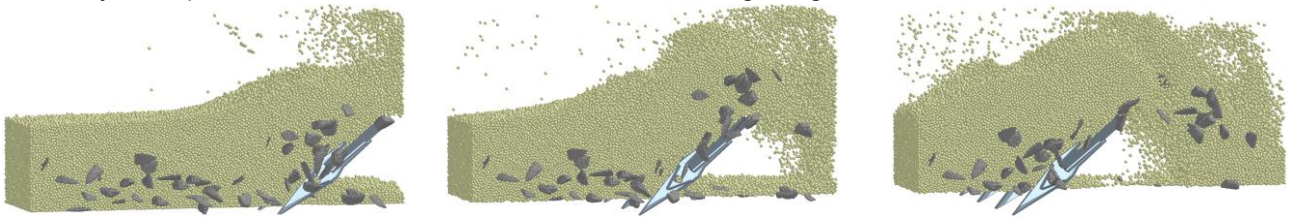

(a) depth = 160 mm *(b) depth = 180 mm* *(c) depth = 200 mm*

Fig. 8 - Rock Particle Motion at Different Working Depths

Table 6

Test factor level design

Serial Number	Angle (°)	REE (%)	Torque (N·m)
1	30°	83.8	315.4
2	40°	79.2	335.9
3	50°	73.9	358.6

Figure 9 illustrates rock particle motion at shovel angles of 30°, 40°, and 50°. At 30° (Fig. 9a), the shovel slides beneath the soil with limited rock engagement and minimal displacement. At 40° (Fig. 9b), the contact between the shovel and buried rocks increases significantly, causing noticeable lifting and separation. However, at 50° (Fig. 9c), the shovel penetrates steeply, pushing rocks laterally with less upward motion, which may reduce extraction efficiency. These results suggest that a moderate angle (around 40°) provides the best balance between penetration and rock-lifting effectiveness.

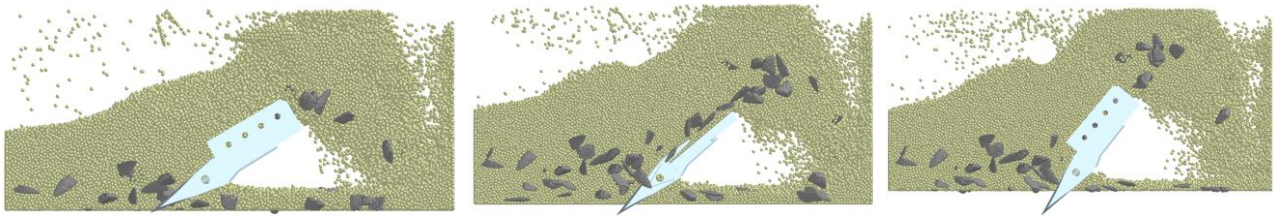

(a) degree = 30° *(b) degree = 40°* *(c) degree = 50°*

Fig. 9 - Rock Particle Motion at Different Working Degree

BBD response surface test results and analysis

To investigate the effects of three independent variables (A, B, and C) on response efficiency (REE) and torque, a Box–Behnken design (BBD) approach was employed. Table 7 presents the experimental design and results, including factor settings (A, B, and C), response efficiency (REE), and torque output.

The results indicate that Serial number 13 (center point with A=B=C=0) achieved the highest REE value (88.1%) and a relatively high torque output (386 N·m), suggesting a potential optimal combination near the center of the design space. In contrast, Serial number 7 (A=0, B=1, C=-1) recorded the lowest REE (64.5%) despite moderate torque (372 N·m), reflecting a condition less favorable for efficient energy utilization.

This variation in REE performance across runs can be attributed to the interaction effects among factors A, B, and C. For example, combinations where B and C had opposing signs (e.g., Serial 7 and 6) tended to show reduced REE, possibly due to conflicting effects on system dynamics. Conversely, center point conditions (Serial 13) may have benefited from a more balanced contribution of each factor, minimizing energy loss while maintaining torque. Additionally, Serial 12 (A=1, B=0, C=1) also produced high torque (421 N·m) with reasonably good REE (74.9%), indicating that positive settings of A and C may be favorable for torque output enhancement.

In conclusion, the BBD test results highlight that the optimal performance-in terms of both REE and torque-is likely located near the design center, and that specific combinations of factor levels significantly affect energy efficiency. These findings provide a basis for response surface modeling and further optimization of system parameters.

Table 7

Design of BBD response surface experiment

Serial number	A	B	C	REE (%)	Torque (N·m)
1	-1	-1	0	80.8	352
2	1	−1	0	74.8	368
3	−1	1	0	68.8	372
4	1	1	0	70.8	420
5	0	−1	−1	76.5	348
6	0	−1	1	69.5	360
7	0	1	−1	64.5	372
8	0	1	1	65.5	408
9	−1	0	−1	79.9	365
10	1	0	−1	76.7	391
11	−1	0	1	75.7	383
12	1	0	1	74.9	421
13	0	0	0	88.1	386

To evaluate the significance of the BBD response surface model and identify the key factors influencing REE, an ANOVA (analysis of variance) was performed. Table 8 presents the results, including the sum of squares, degrees of freedom, mean squares, F-values, and corresponding P-values for each factor and interaction term. The model was found to be highly significant ($P = 0.0005$), with a large F-value (28.53), indicating that the regression model explains a substantial portion of the variation in REE. Among the primary factors, A ($P = 0.0002$), B ($P = 0.0011$), and C ($P = 0.0021$) all showed statistically significant effects, with factor A exhibiting the strongest influence ($F = 57.85$).

In addition, the quadratic terms A^2 ($P = 0.0008$), B^2 ($P = 0.0015$), and C^2 ($P = 0.0043$) were also highly significant, suggesting strong curvature in the response surface and confirming the necessity of including second-order terms in the model. Conversely, the two-factor interaction terms (AB, AC, BC) were not statistically significant ($P > 0.05$), indicating that the combined effects of two factors did not significantly alter REE compared to their individual contributions. The lack-of-fit test was marginally non-significant ($P = 0.0514$), which supports the adequacy of the model, although minor unexplained variation may remain.

In conclusion, the ANOVA results confirm the validity of the BBD model and highlight that the individual and quadratic effects of factors A, B, and C are the main contributors to REE variation, while two-factor interactions are less influential. This justifies the use of a full quadratic model for accurate response prediction and optimization. This contributes a coupled shovel–soil–rock interaction with key design parameters, enabling data-driven optimization of shovel performance in rock-picking operations.

Table 8

BBD Response Surface Analysis Of Variance

Source	Sum of Squares	df	Mean Square	F-Value	P-Value
Model	30251.47	9	3361.27	28.53	0.0005
A	6812.73	1	6812.73	57.85	0.0002
B	4034.6	1	4034.6	34.24	0.0011
C	2961.22	1	2961.22	25.13	0.0021
AB	540.67	1	540.67	4.58	0.072
AC	302.88	1	302.88	2.56	0.1576
BC	612.44	1	612.44	5.2	0.0603
A^2	4908.32	1	4908.32	41.66	0.0008
B^2	3862.19	1	3862.19	32.8	0.0015
C^2	2216.42	1	2216.42	18.81	0.0043
Residual Error	822.7	3	274.23	-	-
Lack of Fit	791.24	2	395.62	18.36	0.0514
Pure Error	31.46	1	31.46	-	-
Total	31074.17	12	-	-	-

The regression equation for torque T based on the Box–Behnken design is expressed as follows:

$$T = 386 + 16A + 18B + 12C + 5A^2 + 8AB + 3AC - 13B^2 + 6BC - 1C^2 \quad (3)$$

where: A represent forward speed (m/s), B - digging depth (mm), C - tool angle (°).

To visualize and interpret the interaction effects of variables A, B, and C on torque (T), 3D response surface plots were generated. Figure 10 illustrates the interactive influence of paired factors on torque while the third factor was held constant.

In Fig. 10(a), when C is fixed at 40°, torque increases steadily with the rise of both A and B, particularly showing a sharp increase at higher values of B. This suggests that B plays a dominant role in enhancing torque under these conditions. In Fig. 10(b), with B fixed at 180, torque again exhibits a strong positive correlation with A, and a nonlinear increasing trend with C, indicating that both A and C positively contribute to torque, though A's effect is more linear and consistent. Lastly, in Fig. 10(c), when A is fixed at 0.5, torque shows a clear curved response surface with respect to B and C, with a pronounced peak in the upper right region of the surface. This confirms a significant interaction between B and C in modulating torque output.

These surface plots are consistent with the ANOVA results, where primary factors A and B were significant, and the B² and C² terms showed strong quadratic effects. Although the interaction terms were not statistically significant in the ANOVA (P > 0.05), the curvature observed in the surfaces, especially in Fig. 10(c), suggests that visual inspection may still reveal synergistic tendencies not captured by isolated significance tests.

In summary, the response surface plots reinforce that A and B are the primary drivers of torque, with B-C interactions exhibiting practical relevance in shaping the torque response.

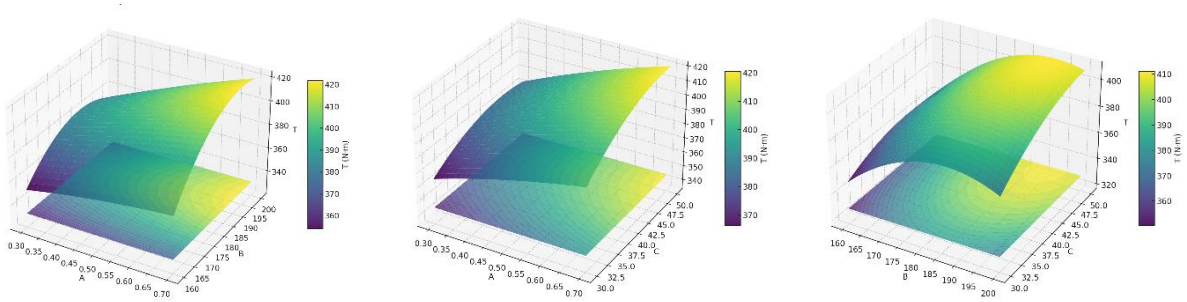

(a) T vs A and B(C = 40°) *(b) T vs A and C (B = 180)* *(c) T vs B and C (A = 0.5)*

Fig. 10 - Influence of the Interaction of Various Factors on the Torque Resistance

Field Performance Verification of the Rock Picker Machine

Fig.11 summarizes the field test results for REE, torque, and their respective errors across three test conditions. Among the three tests, Test 1 demonstrated the most efficient performance**,** combining high metabolic efficiency with stable torque output.

Specifically, Test 1 achieved the highest REE value (89.9%), accompanied by a modest positive REE error (+1.8%), and a torque output of 400.7 N·m with a 3.81% error. In contrast, Test 2 and Test 3 recorded lower REE values (86.2% and 86.7%, respectively), both with negative REE errors (−1.9% and −1.4%), and showed no clear advantage in torque.

Overall, the field test results not only reinforce the optimization trends observed in the simulation but also highlight the model's effectiveness in guiding real-world parameter selection for improved operational performance.

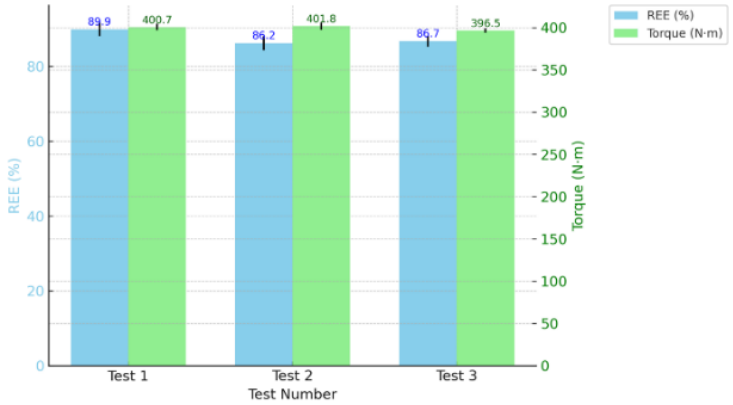

Fig. 11 - REE and Torque Performance Across Field Tests

Figure 12 illustrates the field-testing process and its outcomes. In Fig. 12(a), a tractor-mounted stone removal machine is shown operating in a rocky field, effectively clearing surface debris. Fig. 12(b) displays the result of this operation.

(a) Testing Operation *(b) The Effects Of Testing*

Fig. 12 - The Effects of Field Experiment Operation

Compared with previous studies that applied the Discrete Element Method (DEM) to shovel or soil-tool interaction analysis, this section contributes a more integrated and application-oriented framework. Prior work, such as *Asl and Singh (2009)* and *Zhang et al. (2023)*, focused on optimizing structural parameters-e.g., soil-opening angle, lifting angle, and camber angle-for improved straw burial and reduced resistance in tillage operations. Similarly, *Feng et al. (2022)* investigated DEM-based interactions between excavation tools and granular media on Earth-like terrains to enhance the performance of bucket-type soil removal systems.

Building upon these foundations, the present study expands the modeling scope by incorporating a wider set of physical and contact parameters, including static friction, rolling resistance, and restitution coefficients, which are critical in rock–soil environments. More importantly, these parameters are not only calibrated through simulation but also validated via field experiments-linking micro-scale material behavior with macro-scale equipment performance. This dual-layer validation improves the fidelity of the DEM model, making it more representative of real-world conditions involving complex rock–soil mixtures.

Unlike prior work that emphasized simulation precision in relatively homogeneous or less abrasive materials, this study targets a practical, PTO-driven rock picker operating in rugged agricultural environments. By integrating DEM-based interaction modeling with Box–Behnken Design (BBD) optimization and verifying key performance indicators such as torque and rock extraction efficiency (REE) in field tests, the research offers a systematic and validated approach for structural refinement. Specifically, it provides an effective method for optimizing the shovel design of the 1JS-200 rock picker, addressing both mechanical performance and energy efficiency under realistic working conditions.

CONCLUSIONS

(1) A coupling modeling framework was developed to simulate the interaction between soil, rock, and the lifting shovel using DEM. This model accurately captured the dynamic response of mixed granular media under working conditions and provided a theoretical basis for analyzing force transmission, material flow, and tool loading during rock-picking operations.

(2) A data-driven optimization method based on the Box–Behnken Design (BBD) was established, allowing the investigation of the effects of forward speed, digging depth, and shovel angle on key performance indicators. Response surface models were constructed for both torque and rock excavation efficiency (REE), revealing non-linear relationships and parameter interactions. The optimal parameter combination was determined as a forward speed of 0.5 m/s, a digging depth of 170 mm, and a shovel angle of 40°, under which the REE reached 88.1% with a predicted torque of approximately 386 N·m.

(3) A field validation framework was implemented to verify the simulation-based optimization results. The results of three field trials under the optimal parameter settings showed REE fluctuations within 2% and torque deviations within 4% of the predicted values, confirming the effectiveness and reliability of the model. These findings demonstrate that the optimized shovel design effectively reduces torque load while improving excavation efficiency.

ACKNOWLEDGEMENT

This study was supported by the Open Project of Key Laboratory of Intelligent Agricultural Equipment in Xinjiang (ND2N202302) and the Major Science and Technology Project of Xinjiang Autonomous Region (2022A02007-2-2)

REFERENCES

[1] Asl, J. H., & Singh, S. (2009). Optimization and evaluation of rotary tiller blades: Computer solution of mathematical relations. *Soil and Tillage Research*, 106(1), 1-7.

[2] Camborde, F., Mariotti, C., & Donzé, F. V. (2000). Numerical study of rock and concrete behaviour by discrete element modelling. *Computers and geotechnics*, 27(4), 225-247.

[3] Coetzee, C. J. (2009). The numerical modelling of excavator bucket filling using the discrete element method. *International Journal for Numerical and Analytical Methods in Geomechanics*, 33(11), 1337–1362. https://doi.org/10.1002/nag.771

[4] Coetzee, C. J. (2017). Review: Calibration of the discrete element method. *Powder Technology*, *310*, 104–142. https://doi.org/10.1016/j.powtec.2017.01.015

[5] Cundall, P. A. (1988). Formulation of a three-dimensional distinct element model—Part I. A scheme to detect and represent contacts in a system composed of many polyhedral blocks. In *International journal of rock mechanics and mining sciences & geomechanics abstracts.* Vol. 25, No.3, pp.107-116. Pergamon.

[6] Feng, Y., Wu, J., Guo, C., & Lin, B. (2022). Numerical simulation and experiment on excavating resistance of an electric cable shovel based on EDEM–RecurDyn co-simulation. *Machines*, 10(12), 1203. https://doi.org/10.3390/machines10121203

[7] Fielke, J. U., Ucgul, M., & Saunders, C. (2013). Discrete element modeling of soil-implement interaction considering soil plasticity, cohesion, and adhesion, *Transactions of the ASABE,* Paper No. 131618800. St. Joseph, Mich.: ASABE.

[8] Franco, Y., Rubinstein, D., & Shmulevich, I. (2007). Prediction of soil–bulldozer blade interaction using discrete element method. *Transactions of the ASABE*, 50(1), 345–353. https://doi.org/10.13031/2013.22354

[9] Horn R. Time dependence of soil mechanical properties and pore functions for arable soils[J]. *Soil Science Society of America Journal*, 2004, 68(4): 1131-1137.

[10] Liu, H., Yang, D., & Zhang, X. (2020). Application of discrete element modeling (DEM) for the mechanical analysis of construction materials. *Construction and Building Materials*, 246, 118473. https://doi.org/10.1016/j.conbuildmat.2020.118473

[11] Mak, T., & Chen, Y. (2014). Discrete element modeling of cultivator sweep-to-soil interaction. Journal of *Terramechanics*, 53, 1–10. https://doi.org/10.1016/j.jterra.2014.01.001

[12] Rizzardo, C., Katyara, S., Fernandes, M., & Chen, F. (2020). The importance and the limitations of Sim2Real for robotic manipulation in precision agriculture. *arXiv preprint arXiv:2008.03983*. https://arxiv.org/abs/2008.03983

[13] Shmulevich, I., Asaf, Z., & Rubinstein, D. (2007). Interaction between soil and a wide cutting blade using the discrete element method. *Soil and Tillage Research*, 97(1), 37–50. https://doi.org/10.1016/j.still.2007.08.004

[14] Servin, M., Berglund, T., & Nystedt, S. (2020). A multiscale model of terrain dynamics for real-time earthmoving simulation. *arXiv*. https://arxiv.org/abs/2011.00459

[15] Zou, J., Yang, W., & Han, J. (2020). Discrete element modeling of the effects of cutting parameters and rock properties on rock fragmentation. *IEEE Access*, 8, 136393-136408.

[16] Zhang J, Xia M, Chen W, Yuan D, Wu C, Zhu J. Simulation Analysis and Experiments for Blade-Soil-Straw Interaction under Deep Ploughing Based on the Discrete Element Method. *Agriculture*. 2023; 13(1):136. https://doi.org/10.3390/agriculture13010136

[17] Zhang, Y., & Li, L. (2024). Optimization of discrete element method model to obtain stable and reliable numerical results of mechanical response of granular materials. *Minerals, 14*(8), 758. https://doi.org/10.3390/min14080758